20TH
OPEN ACCESS
ANNIVERSARY

OXFORD

VirBR counter-silences HppX3 to promote conjugation of *bla*~NDM~-IncX3 plasmids

Yuan Gao[1,2,†], **Ning Xie**[1,2,†], **Tengfei Ma**[1,3], **Chun E. Tan**[1,2], **Zhuo Wang**[1,2], **Rong Zhang**[4], **Shizhen Ma**[1,2], **Zhaoju Deng**[2,5,*], **Yang Wang** [1,2,*], **Jianzhong Shen**[1,2,*]

[1]National Key Laboratory of Veterinary Public Health and Safety, College of Veterinary Medicine, China Agricultural University, Beijing 100193, China
[2]Technology Innovation Center for Food Safety Surveillance and Detection (Hainan), Sanya Institute of China Agricultural University, Sanya 572025, China
[3]Institute of Animal Science and Veterinary Medicine, Shandong Academy of Agricultural Sciences, Jinan 250100, China
[4]Clinical Microbiology Laboratory, The Second Affiliated Hospital of Zhejiang University, Zhejiang University, Hangzhou 310009, China
[5]Large Animal Clinical Veterinary Research Center, College of Clinical Medicine, China Agricultural University, Beijing 100193, China

To whom correspondence should be addressed. Email: zhaoju_deng@cau.edu.cn
*Correspondence may also be addressed to Yang Wang. Email: wangyang@cau.edu.cn
Correspondence may also be addressed to Jianzhong Shen. Email: sjz@cau.edu.cn
[†]The first two authors should be regarded as Joint First Authors.

Abstract

New Delhi metallo-β-lactamases (NDM), encoded by the *bla*~NDM~ gene, mediate carbapenem resistance, posing serious threats to public health due to their global presence across diverse hosts and environments. The *bla*~NDM~ is prominently carried by the IncX3 plasmid, which encodes a Type IV secretion system (T4SS) responsible for plasmid conjugation. This T4SS has been shown to be phenotypically silenced by a plasmid-borne H-NS family protein; however, the underlying mechanisms of both silencing and silencing relief remain unclear. Herein, we identified HppX3, an H-NS family protein encoded by the IncX3 plasmid, as a transcription repressor. HppX3 binds to the T4SS promoter (P~actX~), downregulates T4SS expression, thereby inhibits plasmid conjugation. RNA-seq analysis revealed that T4SS genes are co-regulated by HppX3 and VirBR, a transcription activator encoded by the same plasmid. Mechanistically, VirBR acts as a counter-silencer by displacing HppX3 from P~actX~, restoring T4SS expression and promoting plasmid conjugation. A similar counter-silencing mechanism was identified in the T4SSs of IncX1 and IncX2 plasmids. These findings provide new insights into the regulatory mechanisms controlling T4SS expression on multiple IncX plasmids, including the IncX3, explaining the persistence and widespread of *bla*~NDM~-IncX3 plasmid, and highlight potential strategies to combat the spread of NDM-positive *Enterobacterales* by targeting plasmid-encoded regulators.

Graphical abstract
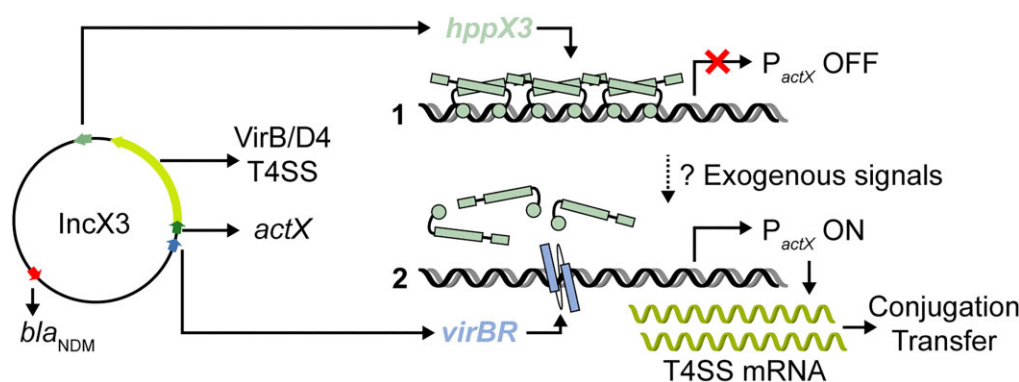
Introduction

The emergence of carbapenem-resistant *Enterobacterales* (CRE) has become a significant health burden due to infections that are difficult to treat [1]. CRE, particularly those producing New Delhi metallo-β-lactamase (NDM)-type carbapenemase, are widely disseminated across humans, animals, and the environment [2, 3]. NDM, encoded by the *bla*~NDM~ gene, hydrolyzes almost all β-lactams, including carbapenems

[4, 5]. Among the 70 identified bla_{NDM} variants (bla_{NDM-1}–bla_{NDM-70}), bla_{NDM-5} and bla_{NDM-1} are the most prevalent, accounting for 74.1% and 16.6% in 1774 NDM-positive *Escherichia coli* strains, respectively [6]. The bla_{NDM} is predominantly carried by the IncX3 plasmid, which has been reported in over 40 countries due to its efficient conjugation and minimal fitness cost to the bacterial host [7–11].

Conjugation plays a critical role in plasmid dissemination [12, 13]. Most IncX3 plasmids possess conjugation machinery that enables their transfer between bacteria via the Type IV secretion system (T4SS), which generally consists of 12 core subunits spanning the bacterial cell envelope [14–17]. Although essential for conjugation, this energy-intensive process imposes a fitness cost on the host bacteria, requiring tight regulation of T4SS expression [18, 19]. Such regulation has been extensively studied in the *tra*-T4SS system of the F plasmid, where expression is activated by the plasmid-borne transcription regulator TraJ and repressed by both the plasmid-encoded fertility inhibition system FinOP and the chromosomal histone-like nucleoid structuring protein (H-NS) [20, 21].

H-NS, a well-studied nucleoid-associated protein in *Enterobacterales*, binds AT-rich DNA regions to form filaments and/or bridges, blocking RNA polymerase (RNAP) access, thereby silencing gene expression and reducing associated fitness costs [22–28]. H-NS is particularly effective at binding mobile genetic elements (MGEs), which are typically AT-rich, helping the integration of some beneficial genes from MGEs into host regulatory circuits [29]. Some MGEs encode H-NS homologs to repress their own genes, minimizing fitness cost, such as Sfh from IncH1 in *Shigella flexneri* and Acr2 from IncA/C in *E. coli* [30–32]. In IncX3, the T4SS is phenotypically repressed by a plasmid-borne H-NS-like protein, although the precise mechanism of this repression remains unclear [33, 34].

To counteract H-NS-mediated gene silencing, bacteria recruit transcription activators or counter-silencers that displace H-NS family proteins from promoter regions, restoring gene expression [35, 36]. For instance, ArcA in *E. coli*, a component of the Arc two-component system, binds the promoters of several virulence genes, countering H-NS repression [37, 38]. Some horizontally acquired elements also encode counter-silencers, such as CsgD from the *csg* locus in *Salmonella* and MxiE protein from virulence plasmid in *S. flexneri* [39, 40]. Similarly, in IncX3, VirBR, a recently identified transcription regulator, activates T4SS expression, thereby enhancing plasmid conjugation [41]. Given that IncX3 conjugation is downregulated by an H-NS-like protein, the role of VirBR as a potential counter-silencer warrants further investigation.

Here, we identified the H-NS-like protein encoded by the IncX3 plasmid, designated HppX3, as a functional member of the H-NS family that binds to both the *E. coli* chromosome and IncX3 plasmid. Specifically, HppX3 binds to the *actX* promoter (P_{actX}), controlling T4SS gene expression, inhibiting plasmid conjugation, and reducing associated fitness cost. We further demonstrated that T4SS is co-regulated by HppX3 and VirBR, with VirBR displacing HppX3 from P_{actX} both *in vivo* and *in vitro*, restoring T4SS expression and enhancing plasmid conjugation. Similar regulatory mechanisms were identified in the T4SSs of IncX1 and IncX2 plasmids. Collectively, these findings offer new insights into the regulation of T4SS on the IncX3 plasmid and may explain the global spreading of bla_{NDM}-IncX3 plasmid.

Materials and methods

Alignment of H-NS homologs

The amino acid sequences of H-NS (NP_415753.1), StpA (NP_417155.1), and Sfx (WP_001282381.1) were selected to align with HppX3 using MAFFT version 7 [42]. The results were visualized with ESPript 3.0 [43], and sequence identity was derived using NCBI Blastp (https://blast.ncbi.nlm.nih.gov/Blast.cgi).

Bacterial strains and gene deletion

Bacterial strains and plasmids used in this study are listed in Supplementary Table S1. *Escherichia coli* strains were cultured in Luria–Bertani (LB) broth with shaking at 200 revolutions per minute (RPM) or on LB agar plates at 37°C or 30°C, depending on the experiment. Antibiotics were added at the following concentrations when necessary: 0.5 mg/l meropenem, 50 mg/l chloromycetin, 50 mg/l apramycin, 50 mg/l kanamycin, 50 mg/l ampicillin, and 50 mg/l sodium azide. Gene deletions (*hppX3*, *h-ns*, *virBR*, and T4SS cluster in p3R-4; $hppX3^{pQD419}$ in pQD419; *sfx* in R6K) were constructed using λ-RED as previous described [44]. Primers used for plasmid construction and gene deletions are listed in Supplementary Table S2.

Chromatin immunoprecipitation sequencing and chromatin immunoprecipitation quantitative polymerase chain reaction

Chromatin immunoprecipitation was performed following previously reported methods, with modifications [35]. Briefly, bacteria were inoculated in 40 ml LB broth with antibiotics, grown for 6 h, and crosslinked with 1% formaldehyde at 37°C for 30 min. Arabinose (20%) was added at a 1:100 volume ratio 2 h before crosslinking when required. Crosslinking was quenched with 1.6 ml of 2.5 M glycine. Cells were washed with phosphate-buffer solution (PBS) three times, and cell pellets were stored at –80°C.

Cells were lysed in B-PER bacterial protein extraction reagent (Thermo Scientific, USA) containing 1% Triton X-100, 1 mM phenylmethylsulfonyl fluoride (PMSF), 50 μg/ml lysozyme and 1 × protease inhibitors (Beyotime, China) at room temperature for 30 min on a HulaMixer. The cell lysates were sonicated with a Covaris M220 sonicator (75 peak power, 5% duty factor, 200 cycles/burst, 8 min duration). After centrifugation at 15 000 RPM for 15 min at 4°C, 20 μl of the supernatant was taken as Input DNA. Immunoprecipitation was performed using anti-FLAG affinity gel (Beyotime, China). Samples were washed with Tris-buffered saline and eluted with 150 μg/ml 3 × FLAG solution at 4°C for 1 h on a HulaMixer. DNA (including Input DNA) was dissociated from the protein using 1.8 mg/ml proteinase K for 2 h at 42°C and incubated for 16 h at 65°C. ChIP and Input DNA was purified using the MinElute polymerase chain reaction (PCR) Purification Kit (Qiagen, Germany). Chromatin immunoprecipitation sequencing (ChIP-seq) was performed by Sinobiocore (China). Sequence enrichment in the ChIP group compared to the input group was calculated using bamCompare (Galaxy Version 3.5.4) and visualized using IGV v2.17.4 [45]. For chromatin immunoprecipitation quantitative PCR (ChIP-qPCR), the *actX* promoter was chosen as the target and the *ompA* gene was the negative control [46]. Primers are listed in Supplementary Table S2. DNA enrichment was quantified

using the "Relative fold enrichment $= 2^{CTInput-CTChIPed}$" [35]. Data were collected from three biological replicates with three technical replicates.

Protein expression and purification

The coding sequences of HppX3 and VirBR were cloned into pET28a vector and expressed in *E. coli* BL21(DE3) cells. Protein expression was induced by adding of 1 mM isopropyl-β-D-thiogalactopyranoside for 12 h at 30°C. Induced cells were harvested, resuspended in lysis buffer (50 mM NaH_2PO_4, 500 mM NaCl, 5 mM imidazole, pH 8.0), and lysed by sonication. Filtered lysates were incubated with Ni Sepharose (Cytiva, USA) for 2 h at 4°C. After washing the resin, the recombinant proteins were eluted with elution buffer (50 mM NaH_2PO_4, 500 mM NaCl, 300 mM imidazole, pH 8.0). Eluted fractions were dialyzed in PBS and concentrated using 5 kDa (His6-VirBR) or 10 kDa (His6-HppX3) cutoff centrifugal filters (Sartorius, Germany). Protein concentrations were measured using a bicinchoninic acid (BCA) assay kit (Thermo Scientific, USA). Purified proteins were snap-frozen in liquid nitrogen and stored at –80°C.

Electrophoretic mobility shift assay

Electrophoretic mobility shift assays (EMSA) was performed using the LightShift Chemiluminescent EMSA Kit (Thermo Scientific, USA), according to previous studies [35, 47]. Biotin-labeled probes were synthetized by Tsingke Biotech (China) based on *actX* promoter sequence. Binding reactions were conducted in 20 μl systems containing 1 nM DNA probe, $1 \times$ Binding buffer, 5% glycerol, 0.05% NP-40, 5 mM $MgCl_2$, and protein. Mixtures were incubated in room temperature for 20 min. In competitive binding assays, a secondary protein was added and incubated in room temperature for another 20 min. Samples were resolved on 4% polyacrylamide gels in $0.5 \times$ Tris–borate–ethylenediaminetetraacetic acid buffer. Probes were transferred to a positively charged nylon membrane and ultraviolet-crosslinked at 120 mJ/cm² for 2 min. Biotin-labeled DNA was detected according to the manufacturer's instructions.

Promoter activity assay

The *actX* promoter in p3R-4, p19SC11DZ17RtetX4, and R6K was fused with the *eGFP* reporter gene in the pUC19 vector. *Escherichia coli* DH5α strains carrying this reporter plasmid were cultured for 6 h, centrifuged, and resuspended in PBS to $OD_{600} = 0.5$. Fluorescence (excitation 488 nm, emission 525 nm) and OD_{600} were measured with a microplate reader (Tecan, Switzerland). Promoter activity was calculated as "Fluorescence intensity = fluorescence value/OD_{600}" [41, 48]. Data were obtained from at least three replicates.

qPCR and RNA-seq analyses

Bacterial cultures (4 ml LB broth, 6 h) were used for total RNA extraction with an RNA isolation kit (Aidlab, China). Reverse transcription was performed using HiScript III All-in-one RT SuperMix (Vazyme, China). qPCR was performed using 60 ng of complementary DNA, Taq Pro Universal SYBR qPCR Master Mix (Vazyme, China), and monitored with a QuantStudio 7 Flex Real-Time PCR System (Applied Biosystems, USA). The *gapA* gene (Gene ID: 947 679) served as an internal control. Data were obtained from four biological replicates with three technical replicates. RNA-seq was conducted by Origingene (China). Differentially expressed genes were visualized with the R package ggplot2 v3.5.1 [49].

Plasmid conjugation assay

Plasmid conjugation was performed by solid mating, with *E. coli* J53 as the recipient strain [50]. Cultures were adjusted to a 0.5 McFarland standard, donor and recipient cells were mixed at a 1:3 volume ratio. A 50 μl sample of the mixture was spotted on microporous membrane on LB agar and incubated at 37°C for 1–3 h. As an exception, for the conjugation of IncX2 plasmid R6K, the mixtures were incubated at 37°C for 16 h. Cells were plated on LB agar containing 100 mg/l sodium azide (for recipients) and 100 mg/l sodium azide with 0.5 mg/l meropenem (for transconjugants harboring IncX3 plasmid) or 100 mg/l sodium azide with 100 mg/l ampicillin (for transconjugants harboring R6K plasmid). Conjugation frequency was calculated as the ratio of transconjugant colony-forming units (CFU) to recipient CFU. Data were obtained from three biological replicates.

Bacterial growth curve and competition experiments *in vitro*

Overnight cultures were adjusted to a 0.5 McFarland standard and diluted at a 1:100 ratio in a 96-well flat-bottom plate (Corning, USA). Plates were incubated at 37°C in a microplate reader (Tecan, Switzerland) with OD_{600} measured every 2 h. Data was obtained from three biological replicates with three technical replicates.

In vitro competition assays followed previous methods [51]. Two pairs of strains were conducted to competition assay: (i) BW25113/p3R-4Δ*hppX3::cat* versus BW25113/p3R-4, (ii) BW25113/p3R-4Δ*hppX3* versus BW25113/p3R-4ΔT4SS::*cat*Δ*hppX3*. Overnight cultures of competitor strains were adjusted to a 0.5 McFarland standard and mixed at a 1:1 volume ratio. Co-cultures were diluted with 1:1000 into fresh LB broth every 24 h. Mixtures at 1, 3, 5 days were plated on LB agars containing 0.5 mg/l meropenem or 0.5 mg/l meropenem with 50 mg/l chloromycetin to count CFU for total cells and BW25113/p3R-4Δ*hppX3::cat* (or BW25113/p3R-4ΔT4SS::*cat*Δ*hppX3*) cells, respectively. The CFU ratio was used to assess bacterial competition capacity. Data were obtained from three biological replicates.

Bioinformation analyses, statistics, and figures

Sequence alignment of IncX3 plasmids was visualized by Easyfig v2.2.5 [52]. The origin-of-transfer (*oriT*) sites were labeled according to [53]. Statistical analyses were performed by GraphPad Prism software v9.3.1, with details provided in the figure legends. Figures were generated by GraphPad Prism software v9.3.1, R v4.4.0, IGV v2.17.4, and Proksee (https://proksee.ca/).

Results

HppX3 is a functional H-NS family protein encoded by the IncX3 plasmid

Escherichia coli encodes two intact chromosome-borne H-NS family proteins, H-NS and its homolog StpA, which shares 58% amino acid (aa) sequence identity and can generally substitute for each other [54, 55]. These proteins contain

two key domains: the N-terminal dimerization and oligomerization domain, and the C-terminal DNA-binding domain, enabling them to bind DNA and silence gene expression [24]. Previous studies have shown that the IncX3-encoded H-NS-like protein, designated HppX3 (H-NS plasmid proteins from incompatibility group X3) [56], represses plasmid conjugation [33, 34], though the mechanism remains unknown. Given that HppX3 shares 47% and 53% aa sequence identity with H-NS and StpA, respectively, we hypothesized that HppX3 functions similarly in DNA-binding and gene silencing (Supplementary Fig. S1).

To investigate the DNA-binding profile of HppX3, we performed ChIP-seq analysis. The *bla*$_{NDM-5}$-IncX3 plasmid p3R-4 from a chicken *E. coli* strain was introduced into *E. coli* K-12 BW25113 (BW25113/p3R-4). The native *hppX3* gene was knocked out (BW25113/p3R-4Δ*hppX3*) and complemented with a *hppX3-FLAG* allele (BW25113/p3R-4Δ*hppX3* + *hppX3-FLAG*), confirming that the FLAG-tag did not interfere with HppX3 function (Supplementary Fig. S2). ChIP-seq analysis of BW25113/p3R-4Δ*hppX3* + *hppX3-FLAG* revealed 321 binding peaks on the chromosome and 3 peaks on p3R-4 (Fig. 1A and B, Dataset S1). Of these, ~62% (198/321) of HppX3 chromosomal binding peaks overlapped with H-NS binding sites (GEO Accession Nos. GSM5511060, GSM5511061), and 64% (206/321) overlapped with StpA binding sites (GEO Accession Nos. GSM5511074, GSM5511075), suggesting that HppX3 may share functions with H-NS and StpA. On the IncX3 plasmid, HppX3 binding was concentrated in AT-rich regions, particularly near the plasmid replication gene *repB* and T4SS gene cluster (Fig. 1B). Notably, HppX3 bound to the elements that contribute to plasmid conjugation transfer, such as relaxosome gene *taxA/C*, promoter of *virB/D4* T4SS (including type IV coupling protein gene *virD4*), and two origin-of-transfer (*oriT*), suggesting its role in regulating conjugation. To further explore the regulatory role of HppX3, we randomly selected ten chromosome-borne and five plasmid-borne genes near the binding peaks for qPCR analysis. The expression of all chromosomal target genes remained unchanged, regardless of HppX3 presence (Fig. 1C). However, all selected plasmid-borne targets were transcriptionally repressed by HppX3 (Fig. 1C), including three T4SS-associated genes *virBR*, *actX*, and *virD4*, indicating that HppX3 is a functional H-NS family protein capable of binding bacterial DNA and may regulate genes involved in IncX3 T4SS.

HppX3 is a transcription repressor of T4SS

To determine whether IncX3 T4SS genes are regulated by HppX3, we performed RNA-seq on a chicken-origin *E. coli* isolate 3R, which contains one chromosome and four plasmids, including p3R-4 (Supplementary Table S3). By comparing transcript levels between the wild-type strain (3R) and an *hppX3* deletion mutant (3RΔ*hppX3*), we identified 58 genes regulated by HppX3 (|log$_2$FoldChange|>2, $P < .05$), with 52 of these genes being repressed (Fig. 2A, Dataset S2). Notably, genes involved in conjugative transfer, including *virBR*, *taxA/C*, *actX*, and T4SS core subunit genes *virB1-11/D4*, were strongly repressed by HppX3. Consequently, deletion of *hppX3* increased the conjugation frequency of the IncX3 plasmid by nearly 2.5 logs ($P < .0001$) in BW25113 and 4 logs ($P < .05$) in 3R, while complementation with HppX3 restored the frequency to wild-type levels (Fig. 2B

and Supplementary Fig. S3). Notably, 63% (33/52) of the genes repressed by HppX3 were located on the IncX3 plasmid, with 37% (19/52) in the chromosome, and none on the other plasmids (Dataset S2). Further, genes on IncX3 exhibited higher fold changes in expression compared to chromosomal genes (Supplementary Fig. S4), indicating that HppX3 exerts a stronger regulatory effect on plasmid-borne genes. These data, along with the qPCR results showing preferential repression of IncX3 genes (Fig. 1C), confirm that HppX3 primarily silences genes on the IncX3 plasmid.

Since T4SS is responsible for plasmid DNA transfer, and the IncX3 T4SS genes (including upstream gene *actX*) are controlled by the promoter of *actX* (P$_{actX}$), we further explored how HppX3 regulates P$_{actX}$ [16, 41]. EMSA using a His6-tagged HppX3 protein confirmed that the biotin-labeled P$_{actX}$ DNA probe shifted to a higher molecular weight when incubated with purified His6-HppX3, in which the N-terminal His6-tag did not impair the function of HppX3 (Supplementary Fig. S2), indicating direct binding between HppX3 and P$_{actX}$ (Fig. 2C). To verify the regulatory role of HppX3, we fused P$_{actX}$ to an *eGFP* reporter gene and observed reduced promoter activity in the presence of HppX3 (Fig. 2D). However, HppX3 lacking the N-terminal dimerization domain (HppX3ΔNTD) failed to repress P$_{actX}$ activity, suggesting that oligomerization is critical for HppX3 function, consistent with other H-NS family regulators [57, 58]. Knocking out *hppX3* led to de-repression of P$_{actX}$, increasing T4SS gene expression and plasmid conjugation frequency (Fig. 2E and B). These results indicate that HppX3 binds directly to P$_{actX}$, repressing T4SS gene transcription, reducing mRNA levels, and inhibiting IncX3 plasmid conjugation.

Conjugative plasmid T4SS systems are usually repressed when not needed, reducing fitness costs and promoting plasmid spreading [19, 59]. As expected, uncontrolled T4SS expression in the *hppX3* mutant imposed a fitness burden on the host, evidenced by slower growth (Fig. 2F) and reduced competitive ability compared to strains carrying the wild-type plasmid (Fig. 2G and Supplementary Fig. S5). Notably, T4SS repression was specific to HppX3 and not mediated by H-NS (Fig. 2E), suggesting that HppX3 acts as a specialized transcription repressor for IncX3 T4SS, alleviating plasmid-associated fitness costs.

HppX3 and VirBR co-regulate the expression of T4SS

Given the high mobility of the IncX3 plasmid, which suggests that the conjugative machinery is not continuously suppressed to minimize fitness costs, we hypothesized that a counter-silencer neutralizes the repressive effects of HppX3. The plasmid-encoded transcription regulator VirBR emerged as a likely candidate to antagonize HppX3 and restore conjugative transfer [41]. In a previous study, we demonstrated that VirBR directly binds to P$_{actX}$, increasing T4SS gene expression and enhancing conjugation transfer. Additionally, both *hppX3* and *virBR* are located on the highly conserved IncX3 plasmid backbone, suggesting they coevolved with the T4SS (Supplementary Fig. S6). Transcriptomic analysis of the 3R strain overexpressing *virBR* (Fig. 3A and B; GSA Accession Nos. CRR1073487-CRR1073489) further confirmed that VirBR activates T4SS genes. Since these same genes are repressed by HppX3, we concluded that T4SS genes are co-regulated by both HppX3 and VirBR (Fig. 3C, Dataset S2).
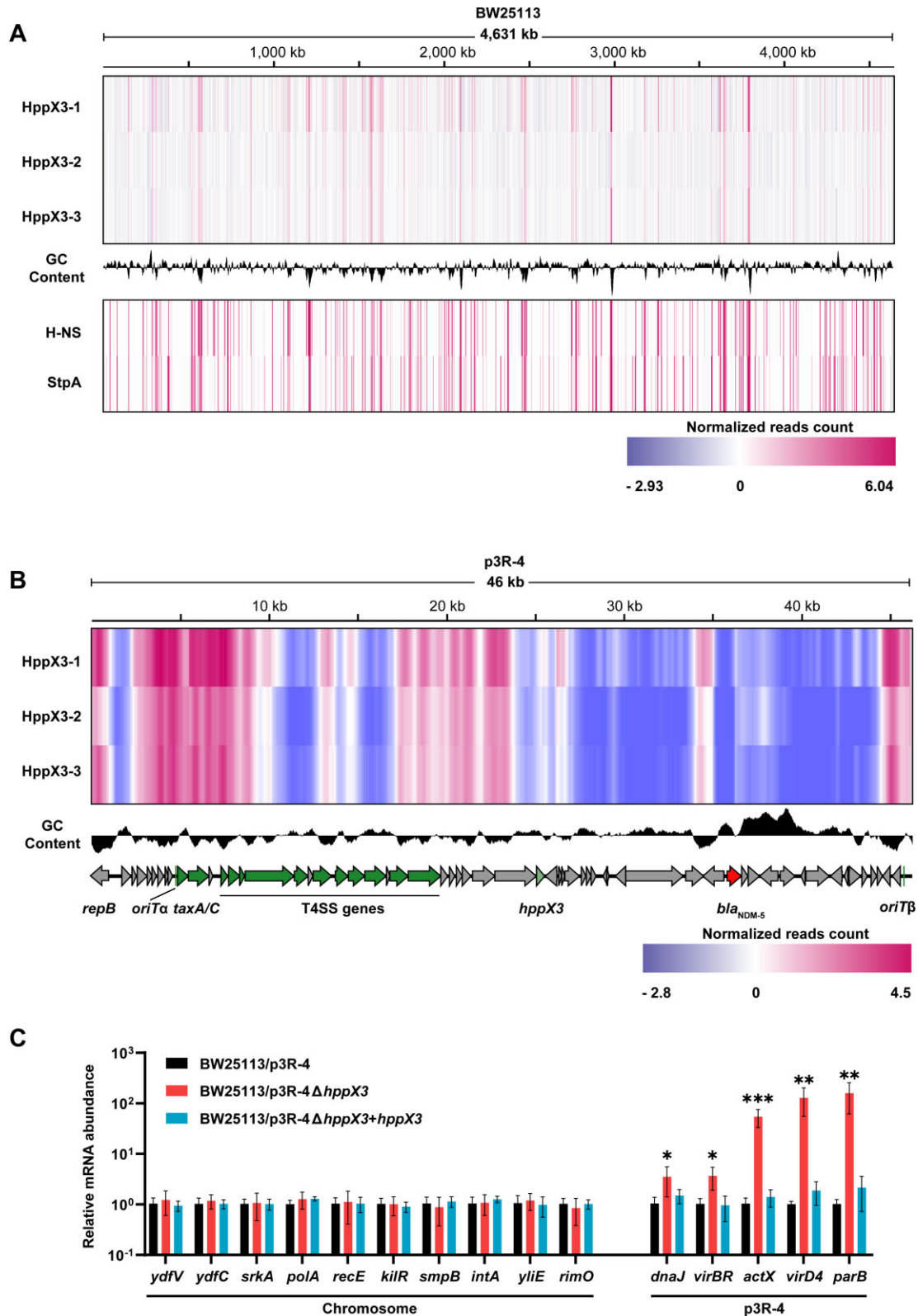
Figure 1. HppX3 binds to bacterial DNA and regulates plasmid genes. (**A**) Comparison of binding peaks of HppX3, H-NS and StpA across BW25113 chromosome. Three biological replicates of HppX3 are presented. (**B**) Binding peaks of three biological replicates of HppX3 across p3R-4 plasmid. The guanine-cytosine (GC) content and annotation of the plasmid sequence are presented below. ChIP-seq profiles, GC content, and sequence annotation were visualized with IGV v2.17.4, Proksee (https://proksee.ca/, window size = 10 000 bp for BW25113 chromosome, window size = 500 bp for p3R-4), and Easyfig v2.2.5, respectively. (**C**) Relative messenger RNA (mRNA) abundance of the randomly selected genes nearby the HppX3 binding peaks on BW25113 chromosome and p3R-4 plasmid, in BW25113/p3R-4 and its derivates. * for $P < .05$, ** for $P < .01$, *** for $P < .001$, compared with "BW25113/p3R-4", based on one way analysis of variance (ANOVA) with Dunnett's multiple comparison test.
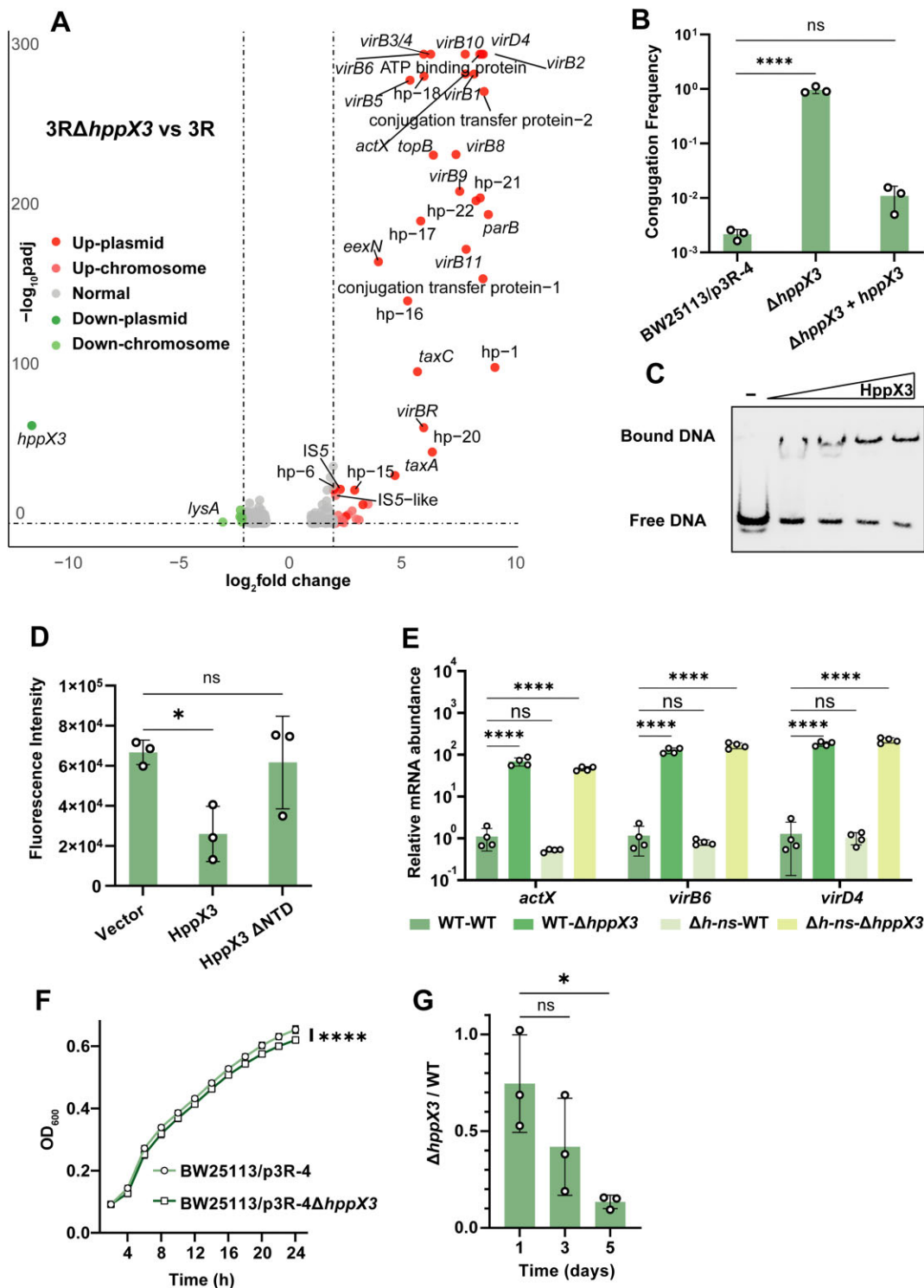
Figure 2. HppX3 repress the expression of T4SS, thereby repressing the plasmid conjugation and plasmid's fitness cost. (**A**) Volcano plot of transcripts for all genes in 3RΔ*hppX3* versus 3R. The differentially expressed genes are represented by different dots. (**B**) Conjugation frequencies of IncX3 plasmid p3R-4 in strains with *hppX3* knocked out or complemented by pACYC184 plasmid. ******** for $P < .0001$, ns for not significant, compared with "BW25113/p3R-4", based on one way ANOVA with Dunnett's multiple comparison test. (**C**) EMSA reactions containing 1 nM biotin-labeled P$_{actX}$ DNA and His6-HppX3 protein (0.4, 0.8, 1.6, 3.2 μg). Lane denotes "−" contained no protein. (**D**) Fluorescence intensity of eGFP under the control of P$_{actX}$. The P$_{actX}$–eGFP is carried by pUC19 vector transformed into *E. coli* DH5α along with pACYC184 carrying *hppX3* and *hppX3*Δ*NTD* (the empty vector was used as a negative control). * for $P < .05$, ns for not significant, compared with "Vector", based on one way ANOVA with Dunnett's multiple comparison test. (**E**) Relative mRNA abundance of *actX*, *virB6*, and *virD4* in BW25113/p3R-4 (wild type-wild type, WT–WT), BW25113/p3R-4Δ*hppX3* (WT-Δ*hppX3*), BW25113Δ*h-ns*/p3R-4 (Δ*h-ns*-WT), and BW25113Δ*h-ns*/p3R-4Δ*hppX3* (Δ*h-ns*-Δ*hppX3*). ******** for $P < .0001$, ns for not significant, compared with "WT–WT", based on one way ANOVA with Dunnett's multiple comparison test. (**F**) Growth curve of BW25113/p3R-4 and BW25113/p3R-4Δ*hppX3*. ******** for $P < .0001$ compared with "BW25113/p3R-4", based on Student's *t*-test for the OD$_{600}$ values at 24 h. (**G**) *In vitro* competition between BW25113/p3R-4Δ*hppX3* (Δ*hppX3*) and BW25113/p3R-4 (WT) in LB broth. * for $P < .05$, ns for not significant, compared with "1 day", based on one way ANOVA with Dunnett's multiple comparison test.
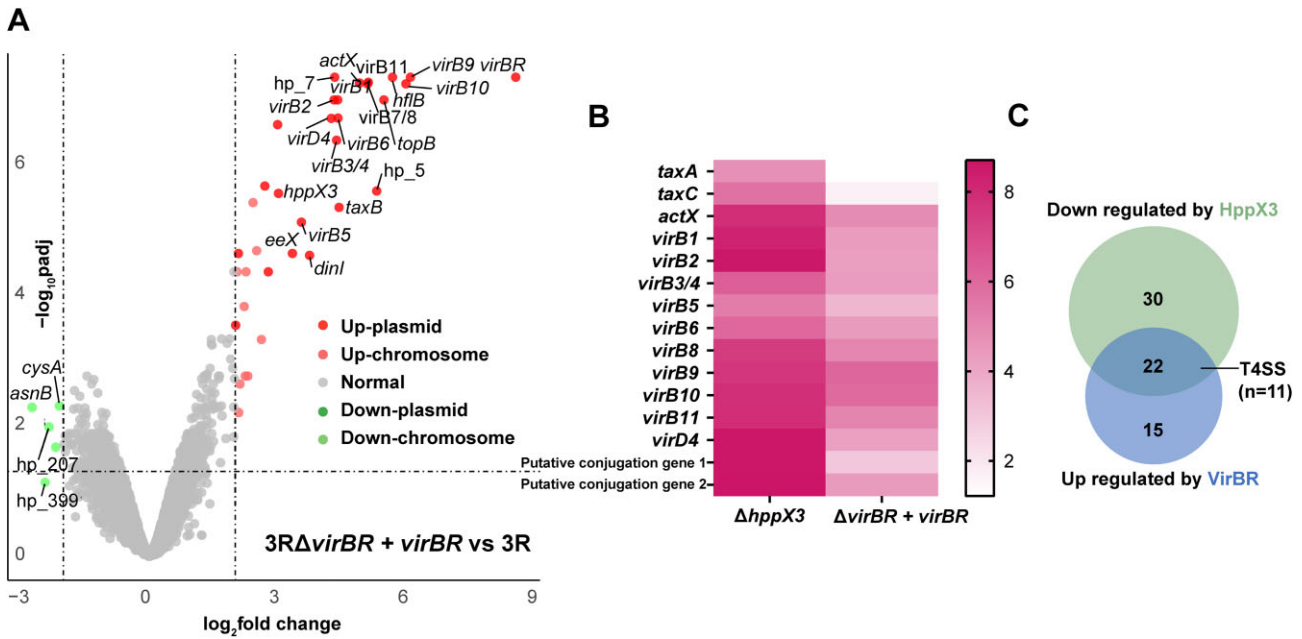
Figure 3. HppX3 and VirBR co-regulate the T4SS. (**A**) Volcano plot of transcripts for all genes in 3RΔ*virBR*/pUC19-*virBR* versus 3R. The differentially expressed genes are represented by different dots. (**B**) Fold changes of conjugation-associated genes in 3RΔ*hppX3* and 3RΔ*virBR*/pUC19-*virBR*, compared with 3R. (**C**) Genes regulated by HppX3 and VirBR according to the RNA-seq data.

We hypothesize that VirBR displaces HppX3 from P$_{actX}$, lifting the repression and allowing T4SS gene expression.

VirBR displaces HppX3 at P$_{actX}$ *in vivo* and *in vitro*

To determine whether VirBR affects the DNA-binding capacity of HppX3 at P$_{actX}$ *in vivo*, we performed ChIP-qPCR. The native *hppX3* in BW25113/p3R-4 was replaced with an *hppX3-FLAG* allele, and *virBR* (or the *RFP* gene as a negative control) was cloned into an arabinose-inducible expression vector pBAD. Overexpression of VirBR resulted in reduced enrichment of P$_{actX}$ DNA, suggesting that HppX3 binds less effectively to P$_{actX}$ in the presence of VirBR (Fig. 4A). Consistently, promoter activity assays showed that VirBR counteracts HppX3's repression of P$_{actX}$ (Fig. 4B). However, when the VirBR binding site within P$_{actX}$ was replaced, VirBR could no longer activate the promoter previously silenced by HppX3, confirming that VirBR's binding to this specific DNA region is essential for counter-silencing (Fig. 4B, lower panel). Further, substituting key amino acids in VirBR (R20, R42, and R67) with alanine (VirBR^M), which disrupts its DNA-binding ability, also prevented the de-repression of the promoter, further emphasizing the necessity of VirBR's binding function (Fig. 4C) [41]. These results demonstrate that VirBR displace HppX3 from P$_{actX}$ *in vivo*.

To confirm this competition between VirBR and HppX3 at P$_{actX}$ *in vitro*, we conducted EMSA using a P$_{actX}$ DNA probe. Increasing concentrations of VirBR progressively shifted the migration pattern of the protein-DNA complex to resemble that of the VirBR-DNA complex alone (Fig. 4D), indicating that VirBR displaces HppX3 from P$_{actX}$ DNA. As expected, de-repression of P$_{actX}$ by VirBR, but not VirBR^M, led to the increased T4SS gene expression and higher conjugation frequency (Fig. 4E and F). Together, these *in vivo* and *in vitro* results provide evidence that VirBR directly competes with HppX3 for binding at the T4SS promoter, displacing HppX3 and alleviating the repression of T4SS gene expression, thus promoting conjugation transfer. Beyond T4SS regulation, VirBR also counter-silenced HppX3 in the regulation of additional potentially functional genes, including *parB* (putative partitioning protein), *ABP* (putative ATP-binding protein), and *topB* (putative type **III** topoisomerase) (Supplementary Fig. S7). These results suggest that the interplay between VirBR and HppX3 plays a broader role in plasmid-associated gene regulation.

The counter-silencing of VirBR-like proteins against H-NS homologs is conserved across multiple IncX plasmids

To determine whether VirBR-mediated counter-silencing of HppX3 is specific to the p3R-4 plasmid, we introduced the *bla*$_{NDM-1}$-IncX3 plasmid pQD419 into *E. coli* BW25113 and knocked out *hppX3*^{pQD419}. Consistent with our observations in p3R-4, deletion of *hppX3*^{pQD419} led to increased T4SS gene expression and enhanced conjugation frequency, while complementation of *hppX3*^{pQD419} restored repression (Fig. 5A and B). Furthermore, introduction of VirBR^{pQD419} alleviated T4SS repression and further promoted the conjugation of pQD419, confirming that VirBR-mediated counter-silencing of HppX3 is conserved in IncX3 plasmids.

Multiple IncX plasmids, including IncX1, IncX2, and IncX3, share homologous T4SS genes and associated regulatory elements [41, 60]. Based on this, we hypothesized that these T4SSs may exhibit similar regulatory mechanisms, where plasmid-encoded H-NS homologs repress T4SS gene expression, and VirBR homologs relieve this repression. To test this, we examined the IncX1 plasmid p19SC11DZ17RtetX4 and IncX2 plasmid R6K (GenBank accession No. LT827129.1). We found that the T4SS promoters of both IncX1 and IncX2 plasmids were repressed by their respective H-NS homologs and were either partially or fully counter-silenced by their VirBR homologs (Fig. 5C and D). To further validate this regulatory mechanism, we knocked
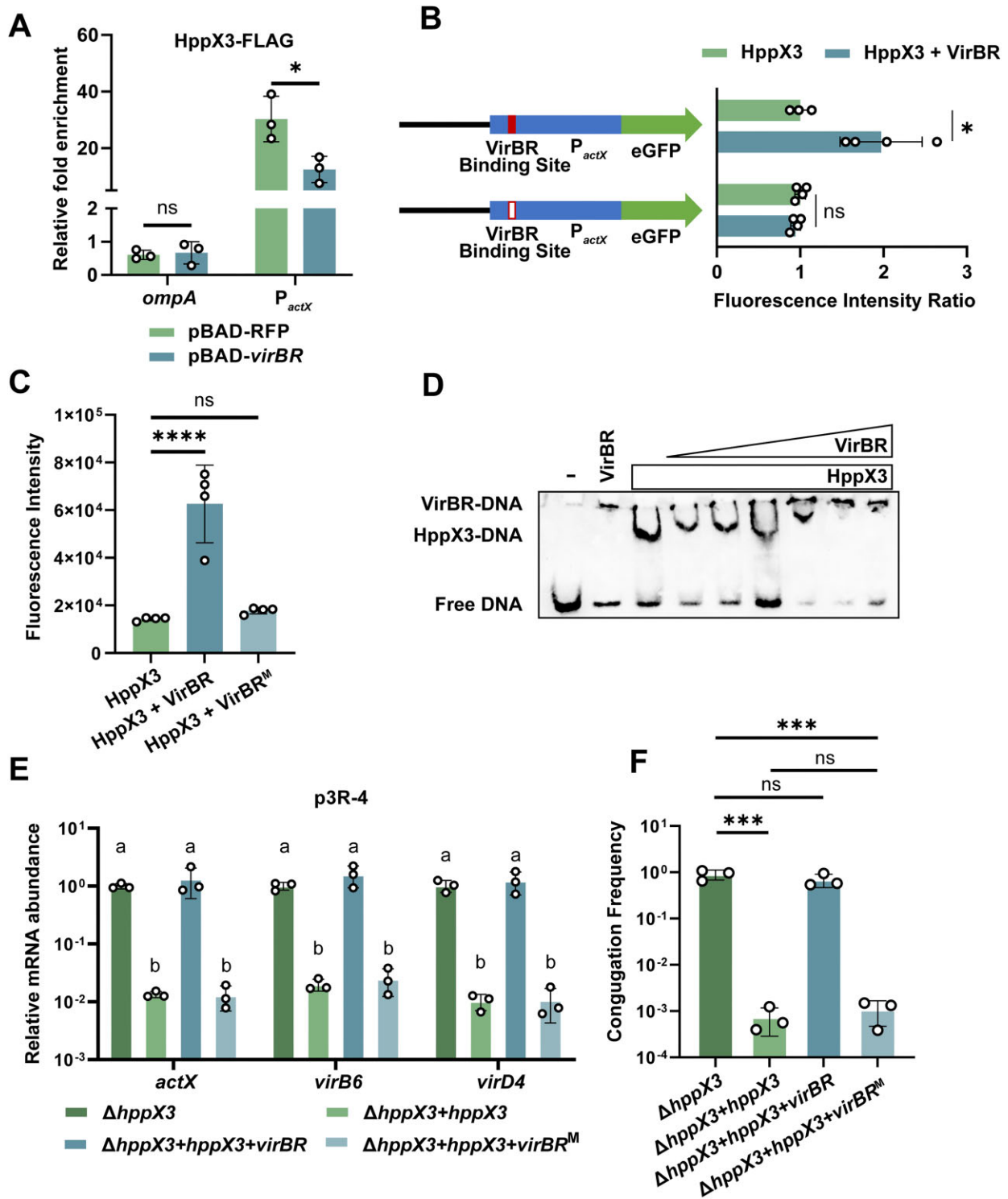
Figure 4. VirBR antagonizes HppX3 at P$_{actX}$. (**A**) *In vivo* binding of HppX3 to the *actX* promoter and *ompA* coding region determined by ChIP-qPCR. The ChIP was conducted in a BW25113/p3R-4 strain that expressing HppX3-FLAG, harboring pBAD-*virBR* or pBAD-RFP (negative control). The ChIP DNA was enriched using anti-FLAG beads and quantified by qPCR. * for *P* < .05, ns for not significant, based on Student's *t*-test. (**B**) Fluorescence intensity of eGFP under the control of P$_{actX}$ or its derivate in the presence of HppX3 with or without VirBR. The *actX* promoter (300-bp-fragment upstream of *actX* start codon) was fused with *eGFP* reporter gene on the pUC19 vector and *hppX3* (or with *virBR*) was cloned into pACYC184 vector. Left panel: Schematic representation of reporter conducts tagged with eGFP, the putative VirBR binding site is marked by solid or hollow blocks. Right panel: Fluorescence intensity ratio normalized to "HppX3" group. * for *P* < .05, ns for not significant, based on Student's *t*-test. (**C**) Fluorescence intensity of eGFP under the control of P$_{actX}$ in the presence of HppX3 with or without VirBR or VirBR^M (R20A, R42A, and R67A). **** for *P* < .0001, ns for not significant, compared with "HppX3", based on one way ANOVA with Dunnett's multiple comparison test. (**D**) EMSA reactions containing 1 nM biotin-labeled P$_{actX}$ DNA, His6-HppX3 protein (0.8 μg) and His6-VirBR protein (0.05, 0.1, 0.2, 0.4, 0.6, 0.8 μg). Lane denotes "−" contained no protein. (**E**) Relative mRNA abundance of *actX*, *virB6*, and *virD4* in BW25113/p3R-4Δ*hppX3* (Δ*hppX3*) and its derivates. Different letters indicate significant differences between strains, based on one way ANOVA with Tukey's multiple comparison test. (**F**) Conjugation frequency of p3R-4Δ*hppX3* plasmid in BW25113 and strains complemented with *hppX3*, *virBR*, or *virBR*^{M}. *** for *P* < .001, ns for not significant, based on one way ANOVA with Tukey's multiple comparison test.
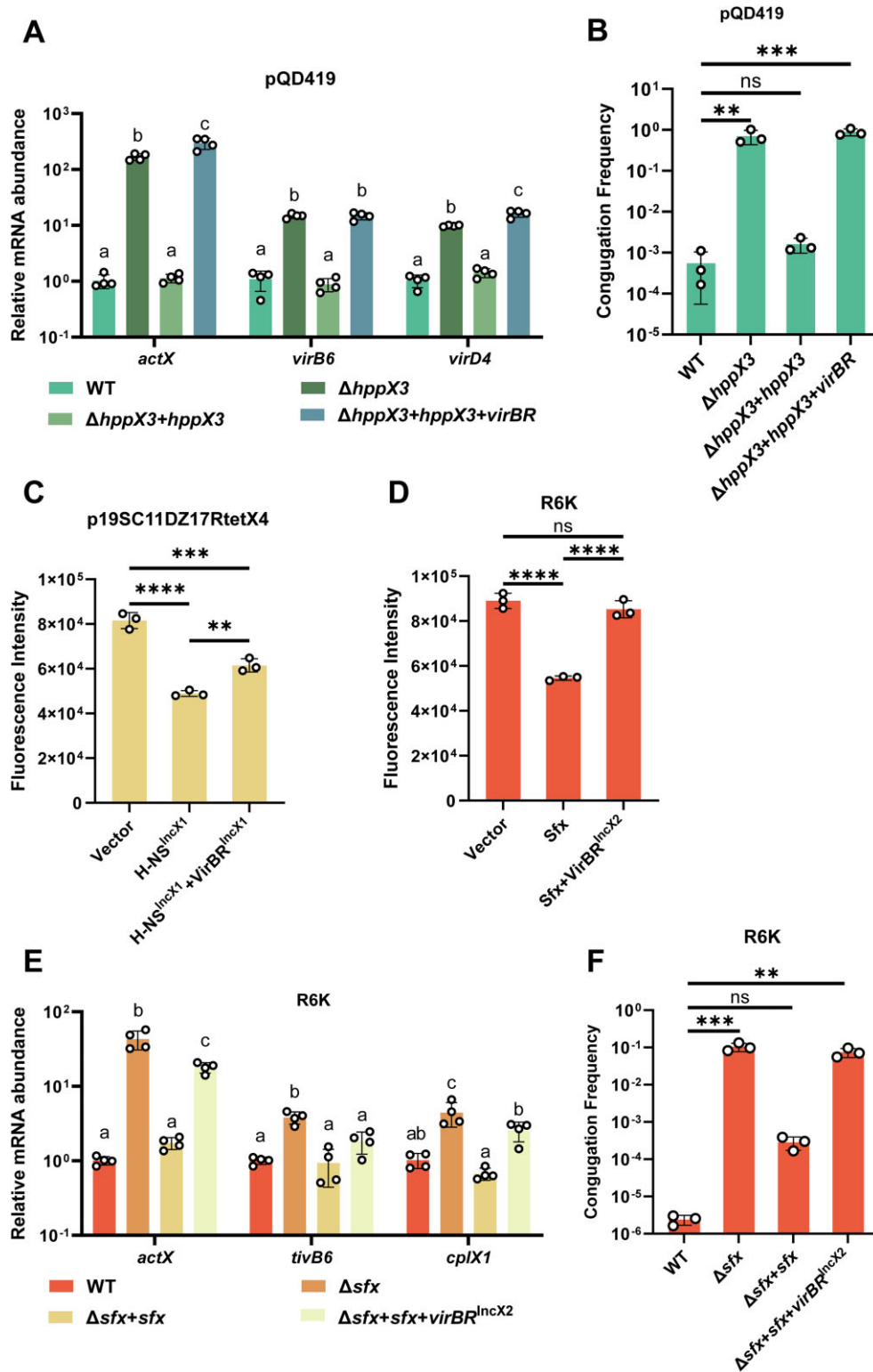
Figure 5. The regulatory interplay between plasmid-borne H-NS family protein and VirBR-like protein is conserved in IncX1, IncX2, and IncX3 plasmids. (**A**) Relative mRNA abundance of *actX*, *virB6*, and *virD4* in BW25113/pQD419 (WT) and its derivates. Different letters indicate significant differences between strains, based on one way ANOVA with Tukey's multiple comparison test. (**B**) Conjugation frequencies of IncX3 plasmid pQD419 in BW25113 (WT) and its derivates. ** for $P < .01$, *** for $P < .001$, ns for not significant, compared with "WT", based on one way ANOVA with Dunnett's multiple comparison test. (**C**) Fluorescence intensity of eGFP under the control of IncX1 T4SS promoter in the presence of H-NS[IncX1] or H-NS[IncX1] and VirBR[IncX1]. ** for $P < .01$, *** for $P < .001$, **** for $P < .0001$, based on one way ANOVA with Tukey's multiple comparison test. (**D**) Fluorescence intensity of eGFP under the control of IncX2 T4SS promoter in the presence of Sfx or Sfx and VirBR[IncX2]. **** for $P < .0001$, ns for not significant, based on one way ANOVA with Tukey's multiple comparison test. (**E**) Relative mRNA abundance of *actX*, *tivB6*, and *cplX1* in BW25113/R6K (WT) and its derivates. Different letters indicate significant differences between strains, based on one way ANOVA with Tukey's multiple comparison test. (**F**) Conjugation frequencies of IncX2 plasmid R6K in BW25113 (WT) and its derivates. ** for $P < .01$, *** for $P < .001$, ns for not significant, compared with "WT", based on one way ANOVA with Dunnett's multiple comparison test.

out the *sfx* gene (encoding the H-NS homolog) in R6K. As expected, deletion of *sfx* increased the T4SS gene expression and conjugation frequency, while complementation restored repression (Fig. 5E,F). As observed in IncX3 plasmids, the introduction of VirBR homolog counter-silenced Sfx, upregulating T4SS gene expression and promoting plasmid conjugation. Collectively, these results demonstrate that the interplay between VirBR-like proteins and H-NS homologs is a conserved regulatory strategy across IncX1, IncX2, and IncX3 plasmids, providing a broad mechanism for controlling T4SS expression and plasmid conjugation in the IncX family.

Discussion

The IncX3 plasmid is the most common vector for antimicrobial resistance genes (ARGs) spreading across the *Enterobacterales* [9]. Despite the prohibition of carbapenem use in animals, bla_{NDM}-IncX3 plasmid-carrying strains have been commonly detected in livestock, farming environments, and manure waste [61]. The ability of IncX3 plasmid to horizontal transfer via conjugation, coupled with its high stability and minimal fitness cost to the bacterial host, has contributed to its global presence [11, 62]. Theoretically, the expression of conjugation-associated T4SS is a major cost of plasmids to their hosts, requiring tight regulation that represses these genes [19, 63]. However, this regulation in IncX3 remains largely unclear. Here we identified HppX3, an H-NS family protein encoded by IncX3 plasmid, as a local transcription repressor of T4SS genes. HppX3 binds to P_{actX} promoter, represses T4SS expression, and downregulates plasmid conjugation. These findings provide deeper insights into the previously reported H-NS-like protein encoded by IncX3 plasmids [33, 34]. The unregulated expression of T4SS in strains lacking HppX3 leads to reduced growth rate and competitiveness, highlighting the essential role of HppX3 in limiting fitness costs of the IncX3 plasmid and promoting its dissemination. Similar to other H-NS family repressors [57, 58], the inability of the HppX3ΔNTD mutant to repress P_{actX} suggests that oligomerization, mediated by the N-terminal domain, is crucial for its gene-silencing function. Additionally, like other H-NS homologs encoded by IncX plasmids, HppX3 contains an RGR AT-hook motif, which may help target specific genes, providing a selective advantage that enhances the regulation of T4SS independent of chromosomal H-NS [58].

MGEs, such as those carrying ARGs and virulence genes, often introduce new traits to their host and must be integrate into host regulatory circuits [64, 65]. During this adaptation, MGEs typically exhibit higher AT-content, which attracts gene silencers like H-NS in proteobacteria to repress their expression and reduce fitness costs [23, 29]. To further minimize their burden, many MGEs encode H-NS analogs that regulate their own genes. Several IncX plasmids have been shown to carry H-NS analogs, such as the H-NS protein in *tet*(X4)-bearing IncX1 plasmids [66], Sfx in IncX2 [58], and HppX3 in IncX3 [33, 34]. These analogs reduce plasmid-associated fitness costs by inhibiting the expression of ARGs or conjugation genes, representing a common strategy for MGEs to adapt to their hosts. Interestingly, recent studies suggest noncanonical functions for H-NS analogs, such as the activation of plasmid partition systems in *Pseudoalteromonas rubra* plasmid pMBL6842, indicating these proteins may play diverse roles in plasmid stability and adaptation [67].

Similar to other plasmids, the IncX3 T4SS mediates plasmid conjugation and promotes the spread of ARGs. The expression of T4SS genes is usually tightly regulated, as exemplified by the well-studied *tra*-T4SS encoded in the F plasmid [20]. Our study, together with previous research, demonstrates that the *virB/D4* T4SS of the IncX3 plasmid is repressed by the gene silencer HppX3 (Fig. 2) [33, 34]. To overcome this repression and activate T4SS expression when needed, bacteria employ counter-silencers such as TraJ in the F plasmid, which cooperates with ArcA [68]. For the *virB/D4* T4SS of IncX3, we show that VirBR, a recently identified transcription regulator, shares regulatory targets with HppX3 and counteracts its silencing, thereby promoting T4SS expression [41]. Notably, this counter-silencing mechanism is not restricted to IncX3 plasmids but is also conserved across multiple IncX subtypes. By extending our investigation to IncX1 and IncX2 plasmids, we identified similar regulatory interactions (Fig. 5C-F). This regulatory conservation underscores the biological importance of precise T4SS control, allowing these plasmids to balance efficient conjugation with minimal fitness cost to their bacterial hosts. This finely tuned mechanism may contribute to the wide dissemination of IncX plasmids and their associated ARGs, thereby playing an essential role in the global spread of multidrug resistance.

The primary mechanism employed by counter-silencers is known as disruptive counter-silencing, where the transcription regulators remodel the H-NS-DNA complex to make gene promoters accessible to RNAP [65, 69]. For example, in *Shigella*, the central virulence regulator VirB binds to the promoters of silenced genes, remodeling DNA supercoils and alleviating gene silencing mediated by H-NS [70]. Some transcription regulators also employ supportive mechanisms, where the counter-silencer not only remodels nucleoprotein complexes but also assists RNAP interaction, as seen with LuxR in *Vibrio harveyi* [35]. In this study, we demonstrate that VirBR interferes with HppX3's DNA-binding both *in vitro* and *in vivo*, relieving the repression of HppX3-silenced genes (Fig. 4). However, when the binding of VirBR to P_{actX} was blocked, either by mutating its binding site or substituting key amino acids (Fig. 4B and C), it could no longer antagonize HppX3, indicating direct competition between these regulators. Although this competitive mechanism is investigated in this study, we observed that the *virBR* deletion partially downregulated T4SS gene expression (by 35%–84%) even in the absence of HppX3 (Supplementary Fig. S8A). This suggests that VirBR may also play a supportive role in T4SS regulation, which warrants further investigation.

Both VirBR and HppX3, belonging to IncX3 plasmid backbone, has remained highly conserved over the past decades, suggesting their evolutionary advantage in regulating T4SS expression [71]. HppX3 switches T4SS "OFF" to minimize fitness cost for host strains, while VirBR turns it "ON" under specific conditions. However, T4SS gene expression in BW25113/p3R-4Δ*virBR* is nearly identical to the wild type (Supplementary Fig. S8A), similar to what was observed with PixR in the IncX4 plasmid [60]. This suggests that *virBR* may be nontranscribable or inactive under laboratory conditions to prevent unnecessary conjugation machinery expression. Our observation that overexpression of *virBR* increases *actX* mRNA levels supports the idea that *virBR* regulation likely occurs at the pre-transcriptional level (Supplementary Fig. S8B). These results highlight gaps in our understanding of IncX3 T4SS regulation,

particularly concerning the signals required to activate T4SS expression.

Generally, T4SS remains "OFF" by default, and specific signals are needed to induce its activation, such as signaling molecules and environmental conditions [19]. Studies suggest that activation of the *Agrobacterium* T4SS, a prototype of the IncX3 T4SS, depends on the host cells-produced opines and quorum signaling molecules [19, 72]. Similarly, activation of *tra*-T4SS in the F plasmid begins with the relief of FinOP-mediated repression [59]. We previously demonstrated that both antibiotic amoxicillin and heavy metals feed additives can act as exogenous stimuli and promote the spreading and colonizing of IncX3-carrying bacteria [41]. Further study is needed to determine whether these signals also affect the "ON/OFF" state of IncX3 T4SS.

This study has certain limitations. First, the upstream regulatory signals controlling *hppX3* expression remains to be elucidated, and further study is needed to determine the factors influencing its transcriptional regulation. Second, this study primarily examines the competition between VirBR and HppX3 in a controlled laboratory setting; however, their regulatory interplay may vary under more complex environmental conditions. Future studies should explore how varied physiological and ecological contexts influence this regulatory mechanism, especially in clinically-relevant settings.

In summary, we identified HppX3, an H-NS family protein encoded by the *bla*$_{NDM-5}$-IncX3 plasmid, as a local gene silencer that represses T4SS expression and minimizes plasmid-associated fitness costs. VirBR serves as a counter-silencer, displacing HppX3 at P$_{actX}$ and promoting T4SS expression and plasmid conjugation. These findings highlight the essential role of plasmid-encoded regulators in adapting and spreading of the *bla*$_{NDM}$-IncX3 plasmid. Given the importance of IncX3 plasmid in the spreading of carbapenemase-encoding genes, unraveling these regulatory mechanisms offers valuable strategies for curbing the global NDM spreading.

Acknowledgements

Supplementary data

Supplementary data is available at NAR online.

Conflict of interest

None declared.

Funding

Data availability

References

1. Bonomo RA, Burd EM, Conly J *et al*. Carbapenemase-producing organisms: a global scourge. *Phil Trans R Soc B* 2018;**66**:1135–48. https://doi.org/10.1093/cid/cix893
2. Rahman MK, Rodriguez-Mori H, Loneragan G *et al*. One health distribution of beta-lactamases in enterobacterales in the United States: a systematic review and meta-analysis. *Int J Antimicrob Agents* 2024;**65**: 107422. https://doi.org/10.1016/j.ijantimicag.2024.107422
3. Fu B, Xu J, Yin D *et al*. Transmission of *bla*$_{NDM}$ in Enterobacteriaceae among animals, food and human. *Emerg Microbes Infect* 2024;**13**:2337678. https://doi.org/10.1080/22221751.2024.2337678
4. Yong D, Toleman MA, Giske CG *et al*. Characterization of a new metallo-beta-lactamase gene, *bla*$_{NDM-1}$, and a novel erythromycin esterase gene carried on a unique genetic structure in *Klebsiella pneumoniae* sequence type 14 from India. *Antimicrob Agents Chemother* 2009;**53**:5046–54. https://doi.org/10.1128/AAC.00774-09
5. Ma J, Song X, Li M *et al*. Global spread of carbapenem-resistant *Enterobacteriaceae*: epidemiological features, resistance mechanisms, detection and therapy. *Microbiol Res* 2023;**266**:127249. https://doi.org/10.1016/j.micres.2022.127249
6. Xia C, Yan R, Liu C *et al*. Epidemiological and genomic characteristics of global *bla*$_{NDM}$-carrying *Escherichia coli*. *Ann Clin Microbiol Antimicrob* 2024;**23**:58. https://doi.org/10.1186/s12941-024-00719-x
7. Dong H, Li Y, Cheng J *et al*. Genomic epidemiology insights on NDM-producing pathogens revealed the pivotal role of plasmids on *bla*$_{NDM}$ transmission. *Microbiol Spectr* 2022;**10**:e0215621. https://doi.org/10.1128/spectrum.02156-21
8. Qin J, Wang Z, Xu H *et al*. IncX3 plasmid-mediated spread of *bla*$_{NDM}$ gene in *Enterobacteriaceae* among children in China. *J Glob Antimicrob Resist* 2024;**37**:199–207. https://doi.org/10.1016/j.jgar.2024.03.021
9. Guo X, Chen R, Wang Q *et al*. Global prevalence, characteristics, and future prospects of IncX3 plasmids: a review. *Front Microbiol* 2022;**13**:979558. https://doi.org/10.3389/fmicb.2022.979558
10. Li Y, Yang Y, Wang Y *et al*. Molecular characterization of *bla*$_{NDM}$-harboring plasmids reveal its rapid adaptation and evolution in the Enterobacteriaceae. *One Health Advances* 2023;**1**:30. https://doi.org/10.1186/s44280-023-00033-9
11. Ma T, Fu J, Xie N *et al*. Fitness cost of *bla*$_{NDM-5}$-carrying p3R-IncX3 plasmids in wild-type NDM-free *Enterobacteriaceae*. *Microorganisms* 2020;**8**:377. https://doi.org/10.3390/microorganisms8030377
12. Lopatkin AJ, Meredith HR, Srimani JK *et al*. Persistence and reversal of plasmid-mediated antibiotic resistance. *Nat Commun* 2017;**8**:1689. https://doi.org/10.1038/s41467-017-01532-1
13. Alonso-Del VA, Toribio-Celestino L, Quirant A *et al*. Antimicrobial resistance level and conjugation permissiveness

shape plasmid distribution in clinical enterobacteria. *Proc Natl Acad Sci USA* 2023;**120**:e1980832176.

14. Johnson TJ, Bielak EM, Fortini D *et al.* Expansion of the IncX plasmid family for improved identification and typing of novel plasmids in drug-resistant *Enterobacteriaceae*. *Plasmid* 2012;**68**:43–50. https://doi.org/10.1016/j.plasmid.2012.03.001

15. Cabezón E, Ripoll-Rozada J, Peña A *et al.* Towards an integrated model of bacterial conjugation. *FEMS Microbiol Rev* 2015;**39**:81–95.

16. Costa T, Harb L, Khara P *et al.* Type IV secretion systems: advances in structure, function, and activation. *Mol Microbiol* 2021;**115**:436–52. https://doi.org/10.1111/mmi.14670

17. Christie PJ, Atmakuri K, Krishnamoorthy V *et al.* Biogenesis, architecture, and function of bacterial type IV secretion systems. *Annu Rev Microbiol* 2005;**59**:451–85. https://doi.org/10.1146/annurev.micro.58.030603.123630

18. Peña A, Arechaga I. Molecular motors in bacterial secretion. *J Mol Microbiol Biotechnol* 2013;**23**:357–69.

19. Koraimann G, Wagner MA. Social behavior and decision making in bacterial conjugation. *Front Cell Infect Microbiol* 2014;**4**:54. https://doi.org/10.3389/fcimb.2014.00054

20. Virolle C, Goldlust K, Djermoun S *et al.* Plasmid transfer by conjugation in gram-negative bacteria: from the cellular to the community level. *Genes (Basel)* 2020;**11**:1239. https://doi.org/10.3390/genes11111239

21. Willetts N. The transcriptional control of fertility in F-like plasmids. *J Mol Biol* 1977;**112**:141–8. https://doi.org/10.1016/S0022-2836(77)80161-7

22. Dorman CJ. H-NS: a universal regulator for a dynamic genome. *Nat Rev Micro* 2004;**2**:391–400. https://doi.org/10.1038/nrmicro883

23. Navarre WW, Porwollik S, Wang Y *et al.* Fang FC. Selective silencing of foreign DNA with low GC content by the H-NS protein in *Salmonella*. *Science* 2006;**313**:236–8. https://doi.org/10.1126/science.1128794

24. Grainger DC. Structure and function of bacterial H-NS protein. *Biochem Soc Trans* 2016;**44**:1561–9. https://doi.org/10.1042/BST20160190

25. Shin M, Song M, Rhee JH *et al.* DNA looping-mediated repression by histone-like protein H-NS: specific requirement of Esigma70 as a cofactor for looping. *Genes Dev* 2005;**19**:2388–98. https://doi.org/10.1101/gad.1316305

26. Shin M, Lagda AC, Lee JW *et al.* Gene silencing by H-NS from distal DNA site. *Mol Microbiol* 2012;**86**:707–19. https://doi.org/10.1111/mmi.12012

27. Haycocks JR, Sharma P, Stringer AM *et al.* The molecular basis for control of ETEC enterotoxin expression in response to environment and host. *PLoS Pathog* 2015;**11**:e1004605. https://doi.org/10.1371/journal.ppat.1004605

28. Dole S, Nagarajavel V, Schnetz K. The histone-like nucleoid structuring protein H-NS represses the *Escherichia coli bgl* operon downstream of the promoter. *Mol Microbiol* 2004;**52**:589–600. https://doi.org/10.1111/j.1365-2958.2004.04001.x

29. Dorman CJ. H-NS, the genome sentinel. *Nat Rev Micro* 2007;**5**:157–61. https://doi.org/10.1038/nrmicro1598

30. Doyle M, Fookes M, Ivens A *et al.* An H-NS-like stealth protein aids horizontal DNA transmission in bacteria. *Science* 2007;**315**:251–2. https://doi.org/10.1126/science.1137550

31. Dillon SC, Cameron AD, Hokamp K *et al.* Genome-wide analysis of the H-NS and sfh regulatory networks in *Salmonella* Typhimurium identifies a plasmid-encoded transcription silencing mechanism. *Mol Microbiol* 2010;**76**:1250–65. https://doi.org/10.1111/j.1365-2958.2010.07173.x

32. Lang KS, Johnson TJ. Characterization of Acr2, an H-NS-like protein encoded on A/C2-type plasmids. *Plasmid* 2016;**87-88**:17–27. https://doi.org/10.1016/j.plasmid.2016.07.004

33. Liu B, Shui L, Zhou K *et al.* Impact of plasmid-encoded H-NS-like protein on bla_{NDM-1}-bearing IncX3 plasmid in *Escherichia coli*. *J Infect Dis* 2020;**221**:S229–36. https://doi.org/10.1093/infdis/jiz567

34. Baomo L, Lili S, Moran RA *et al.* Temperature-regulated IncX3 plasmid characteristics and the role of plasmid-encoded H-NS in thermoregulation. *Front Microbiol* 2021;**12**:765492. https://doi.org/10.3389/fmicb.2021.765492

35. Chaparian RR, Tran M, Miller CL *et al.* van Kessel JC. Global H-NS counter-silencing by LuxR activates quorum sensing gene expression. *Nucleic Acids Res* 2020;**48**:171–83.

36. Hustmyer CM, Wolfe MB, Welch RA *et al.* RfaH counter-silences inhibition of transcript elongation by H-NS-StpA nucleoprotein filaments in pathogenic *Escherichia coli*. *mBio* 2022;**13**:e0266222. https://doi.org/10.1128/mbio.02662-22

37. Jiang F, Yang Y, Mao Z *et al.* ArcA positively regulates the expression of virulence genes and contributes to virulence of porcine Shiga toxin-producing enterotoxigenic *Escherichia coli*. *Microbiol Spectr* 2023;**11**:e0152523. https://doi.org/10.1128/spectrum.01525-23

38. Lynch AS, Lin EC. Transcriptional control mediated by the ArcA two-component response regulator protein of *Escherichia coli*: characterization of DNA binding at target promoters. *J Bacteriol* 1996;**178**:6238–49. https://doi.org/10.1128/jb.178.21.6238-6249.1996

39. Newman SL, Will WR, Libby SJ *et al.* The curli regulator CsgD mediates stationary phase counter-silencing of *csgBA* in *Salmonella* Typhimurium. *Mol Microbiol* 2018;**108**:101–14. https://doi.org/10.1111/mmi.13919

40. Hall CP, Jadeja NB, Sebeck N *et al.* Characterization of MxiE- and H-NS-dependent expression of *ipaH7.8*, *ospC1*, *yccE*, and *yfdF* in *Shigella flexneri*. *mSphere* 2022;**7**:e0048522. https://doi.org/10.1128/msphere.00485-22

41. Ma T, Xie N, Gao Y *et al.* VirBR, a transcription regulator, promotes IncX3 plasmid transmission, and persistence of bla_{NDM-5} in zoonotic bacteria. *Nat Commun* 2024;**15**:5498. https://doi.org/10.1038/s41467-024-49800-1

42. Katoh K, Rozewicki J, Yamada KD. MAFFT online service: multiple sequence alignment, interactive sequence choice and visualization. *Brief Bioinform* 2019;**20**:1160–6. https://doi.org/10.1093/bib/bbx108

43. Robert X, Gouet P. Deciphering key features in protein structures with the new ENDscript server. *Nucleic Acids Res* 2014;**42**:W320–4. https://doi.org/10.1093/nar/gku316

44. Datsenko KA, Wanner BL. One-step inactivation of chromosomal genes in *Escherichia coli* K-12 using PCR products. *Proc Natl Acad Sci USA* 2000;**97**:6640–5. https://doi.org/10.1073/pnas.120163297

45. Robinson JT, Thorvaldsdóttir H, Winckler W *et al.* Integrative genomics viewer. *Nat Biotechnol* 2011;**29**:24–6. https://doi.org/10.1038/nbt.1754

46. Choi J, Schmukler M, Groisman EA. Degradation of gene silencer is essential for expression of foreign genes and bacterial colonization of the mammalian gut. *Proc Natl Acad Sci USA* 2022;**119**:e2084728177. https://doi.org/10.1073/pnas.2210239119

47. Ma R, Liu Y, Gan J *et al.* Xenogeneic nucleoid-associated EnrR thwarts H-NS silencing of bacterial virulence with unique DNA binding. *Nucleic Acids Res* 2022;**50**:3777–98. https://doi.org/10.1093/nar/gkac180

48. Walker KA, Miner TA, Palacios M *et al.* A *Klebsiella pneumoniae* regulatory mutant has reduced capsule expression but retains hypermucoviscosity. *mBio* 2019;**10**:e00089-19. https://doi.org/10.1128/mBio.00089-19

49. Wickham H. *ggplot2: Elegant Graphics for Data Analysis*. New York: Springer-Verlag, 2016

50. Wang Y, Zhang R, Li J *et al.* Comprehensive resistome analysis reveals the prevalence of NDM and MCR-1 in Chinese poultry production. *Nat Microbiol* 2017;**2**:16260. https://doi.org/10.1038/nmicrobiol.2016.260

51. Yang J, Wang HH, Lu Y *et al*. A ProQ/FinO family protein involved in plasmid copy number control favours fitness of bacteria carrying *mcr-1*-bearing IncI2 plasmids. *Nucleic Acids Res* 2021;**49**:3981–96. https://doi.org/10.1093/nar/gkab149

52. Sullivan MJ, Petty NK, Beatson SA. Easyfig: a genome comparison visualizer. *Bioinformatics* 2011;**27**:1009–10. https://doi.org/10.1093/bioinformatics/btr039

53. Avila P, Núñez B, de l *et al*. Plasmid R6K contains two functional *oriTs* which can assemble simultaneously in relaxosomes *in vivo*. *J Mol Biol* 1996;**261**:135–43. https://doi.org/10.1006/jmbi.1996.0447

54. Sonden B, Uhlin BE. Coordinated and differential expression of histone-like proteins in *Escherichia coli*: regulation and function of the H-NS analog StpA. *EMBO J* 1996;**15**:4970–80. https://doi.org/10.1002/j.1460-2075.1996.tb00877.x

55. Uyar E, Kurokawa K, Yoshimura M *et al*. Differential binding profiles of StpA in wild-type and h-ns mutant cells: a comparative analysis of cooperative partners by chromatin immunoprecipitation-microarray analysis. *J Bacteriol* 2009;**191**:2388–91. https://doi.org/10.1128/JB.01594-08

56. Fitzgerald S, Kary SC, Alshabib EY *et al*. Redefining the H-NS protein family: a diversity of specialized core and accessory forms exhibit hierarchical transcriptional network integration. *Nucleic Acids Res* 2020;**48**:10184–98. https://doi.org/10.1093/nar/gkaa709

57. Ueguchi C, Seto C, Suzuki T *et al*. Clarification of the dimerization domain and its functional significance for the *Escherichia coli* nucleoid protein H-NS. *J Mol Biol* 1997;**274**:145–51. https://doi.org/10.1006/jmbi.1997.1381

58. Wang A, Cordova M, Navarre WW. Evolutionary and functional divergence of Sfx, a plasmid-encoded H-NS homolog, underlies the regulation of IncX plasmid conjugation. *mBio* 2024;**16**:e0208924. https://doi.org/10.1128/mbio.02089-24

59. Frost LS, Koraimann G. Regulation of bacterial conjugation: balancing opportunity with adversity. *Future Microbiol* 2010;**5**:1057–71. https://doi.org/10.2217/fmb.10.70

60. Yi L, Durand R, Grenier F *et al*. PixR, a novel activator of conjugative transfer of IncX4 resistance plasmids, mitigates the fitness cost of *mcr-1* carriage in *Escherichia coli*. *mBio* 2022;**13**:e0320921. https://doi.org/10.1128/mbio.03209-21

61. Guo CH, Chu MJ, Liu T *et al*. High prevalence and transmission of *bla*NDM-positive *Escherichia coli* between farmed ducks and slaughtered meats: an increasing threat to food safety. *Int J Food Microbiol* 2024;**424**:110850. https://doi.org/10.1016/j.ijfoodmicro.2024.110850

62. Tian D, Wang B, Zhang H *et al*. Dissemination of the *bla*NDM-5 gene via IncX3-type plasmid among *Enterobacteriaceae* in children. *mSphere* 2020;**5**:e00699-19. https://doi.org/10.1128/mSphere.00699-19

63. Dahlberg C, Chao L. Amelioration of the cost of conjugative plasmid carriage in *Eschericha coli* K12. *Genetics* 2003;**165**:1641–9. https://doi.org/10.1093/genetics/165.4.1641

64. Ochman H, Lawrence JG, Groisman EA. Lateral gene transfer and the nature of bacterial innovation. *Nature* 2000;**405**:299–304. https://doi.org/10.1038/35012500

65. Will WR, Navarre WW, Fang FC. Integrated circuits: how transcriptional silencing and counter-silencing facilitate bacterial evolution. *Curr Opin Microbiol* 2015;**23**:8–13. https://doi.org/10.1016/j.mib.2014.10.005

66. Cai W, Tang F, Jiang L *et al*. Histone-like nucleoid structuring protein modulates the fitness of *tet*(X4)-bearing IncX1 plasmids in gram-negative bacteria. *Front Microbiol* 2021;**12**:763288. https://doi.org/10.3389/fmicb.2021.763288

67. Li B, Ni S, Liu Y *et al*. The histone-like nucleoid-structuring protein encoded by the plasmid pMBL6842 regulates both plasmid stability and host physiology of *Pseudoalteromonas rubra* SCSIO 6842. *Microbiol Res* 2024;**286**:127817. https://doi.org/10.1016/j.micres.2024.127817

68. Lu J, Peng Y, Wan S *et al*. Cooperative function of TraJ and ArcA in regulating the F plasmid *tra* operon. *J Bacteriol* 2019;**201**:e00448-18. https://doi.org/10.1128/JB.00448-18

69. Caramel A, Schnetz K. Lac and lambda repressors relieve silencing of the *Escherichia coli bgl* promoter. Activation by alteration of a repressing nucleoprotein complex. *J Mol Biol* 1998;**284**:875–83. https://doi.org/10.1006/jmbi.1998.2191

70. Picker MA, Karney M, Gerson TM *et al*. Localized modulation of DNA supercoiling, triggered by the *Shigella* anti-silencer VirB, is sufficient to relieve H-NS-mediated silencing. *Nucleic Acids Res* 2023;**51**:3679–95. https://doi.org/10.1093/nar/gkad088

71. Liu B, Guo Y, Liu N *et al*. In silico evolution and comparative genomic analysis of IncX3 plasmids isolated from China over ten years. *Front Microbiol* 2021;**12**:725391. https://doi.org/10.3389/fmicb.2021.725391

72. White CE, Winans SC. Cell-cell communication in the plant pathogen *agrobacterium tumefaciens*. *Philos Trans R Soc Lond B Biol Sci* 2007;**362**:1135–48. https://doi.org/10.1098/rstb.2007.2040